Abnormal epigenetic regulation of the gene expression levels of *Wnt2b* and *Wnt7b*: Implications for neural tube defects

BAOLING BAI, SHUYUAN CHEN, QIN ZHANG, QIAN JIANG and HUILI LI

Beijing Municipal Key Laboratory of Child Development and Nutriomics,
Capital Institute of Pediatrics, Beijing 100020, P.R. China

Abstract. The association between *Wnt* genes and neural tube defects (NTDs) is recognized, however, it remains to be fully elucidated. Our previous study demonstrated that epigenetic mechanisms are affected in human NTDs. Therefore, the present study aimed to evaluate whether *Wnt2b* and *Wnt7b* are susceptible to abnormal epigenetic modification in NTDs, using chromatin immunoprecipitation assays to evaluate histone enrichments and the MassARRAY platform to detect the methylation levels of target regions within Wnt genes. The results demonstrated that the transcriptional activities of *Wnt2b* and *Wnt7b* were abnormally upregulated in mouse fetuses with NTDs and, in the GC-rich promoters of these genes, histone 3 lysine 4 (H3K4) acetylation was enriched, whereas H3K27 trimethylation was reduced. Furthermore, several CpG sites in the altered histone modification of target regions were significantly hypomethylated. The present study also detected abnormal epigenetic modifications of these *Wnt* genes in human NTDs. In conclusion, the present study detected abnormal upregulation in the levels of *Wnt2b* and *Wnt7b*, and hypothesized that the alterations may be due to the ectopic opening of chromatin structure. These results improve understanding of the dysregulation of epigenetic modification of *Wnt* genes in NTDs.

Introduction

Abnormal alterations in *Wnt* genes are associated with neural tube defects (NTDs) (1,2). NTDs occur when the neural tube fails to close at the early stage of neural development, which can result in spina bifida, myelomeningocele (also known as spina bifida aperta), exencephaly or craniorachischisis (3). A previous study demonstrated that a null mutation of *Wnt3a*, a canonical *Wnt*, led to spina bifida aperta in mice (4). *Wnt5a⁻/⁻*, a non-canonical *Wnt*, mice did not suffer from NTDs; however, mice with double deletions of the *Wnt5a⁻/⁻* and *Ltap*/*Vangl2* genes exhibited craniorachischisis (5). Furthermore, knockout mutations of the canonical *Wnt3* or non-canonical *Wnt* genes, *Wnt5a and Wnt7a*, induce deformities of the anteroposterior (A/P) axis of the neural tube (6). These findings suggest that, in addition to roles of several known *Wnt* genes in the etiology of NTDs, other *Wnt* members may be involved in the pathogenesis of NTDs.

Wnt2b is a canonical *Wnt*, which is expressed in the primitive streak at embryonic day (E) 7-7.75, followed by the dorsal midline of the telencephalon and mesencephalon at E8.5-9.5, and in the cortical hem at E11.5-17.5 in murine embryos. This specific spatio-temporal expression of *Wnt2b* suggests that it functions in gastrulation, neurulation and cerebral cortex patterning (7,8). In addition, *Wnt7b*, which is associated with canonical and non-canonical *Wnt* signaling, is expressed at E5.5, and is expressed in the forebrain, and the ventral and intermediate spinal cord at the developmental stages during which patterning and neural specification occur (9). Notably, *Wnt7b* can assist in ensuring correct A/P guidance, and is involved in dorsoventral patterning of the amphibian embryonic neural tube (10). Although *Wnt2b* and *Wnt7b* mutations have not induced NTDs in mice (6), they are essential during neural tube patterning; therefore, the present study hypothesized that the expression levels of these two genes are likely to be disrupted in NTDs.

Epigenetic modifications typically regulate gene expression; histone 3 lysine 4 acetylation (H3K4ac) and trimethylation of H3 lysine 4 (H3K4me3), are commonly located in active promoters and are associated with gene activation, whereas H3K27me3 suppresses transcription (11). DNA methylation is predominantly catalyzed by DNA methyltransferase through the addition of a methyl group to cytosine residues on dinucleotide CpG islands, and is frequently distributed in the core promoter close to the transcription start site (TSS); once the promoter CpG islands are methylated, these genes are often transcriptionally inactivated (12). Our previous studies demonstrated that epigenetic modifications were significantly altered in patients with NTDs (13,14); however, the detailed mechanism and target genes remain to be elucidated.

The present study aimed to investigate dysregulation of epigenetic modification of *Wnt* genes in NTDs, using a mouse

model of spina bifida. It was hypothesized that in NTDs, dysregulation of epigenetic modification is involved in the regulation of *Wnt2b* and *Wnt7b* gene expression.

Materials and methods

Animals. All animals experiments were performed in accordance with the standards of the Capital Institute of Pediatrics Ethics Committee (Beijing, China; permit no. SYXK 2008-0011). A total of 40 adult C57BL/6J mice (20 male and 20 female) were housed in light- and temperature-controlled rooms (12/12 h light/dark cycle; 23±1°C) and maintained on pure mouse feed and tap water provided *ad libitum*. Adult virgin females (above 9 weeks of age and 21 g in weight) were mated for 2 h with males (1 male per 2 females, 8:00-10:00 am) of the same stock. A vaginal plug observed at 10:00 AM was considered as embryonic day 0 (E0). The mice were administered with a 20 mg/kg body weight dose of retinoic acid (RA; suspended in olive oil; Sigma-Aldrich, St. Louis, MO, USA) on E8.0-0 h, E8.0-6 h and E8.0-12 h. Mice treated with isovolumetric pure olive oil (Agric, Crete, Greece) at these same time points served as control groups, as described in our previous study (15). E18.0 fetuses were delivered by cesarean section, and 21 cases of spina bifida were selected (Fig. 1A and B). As the spinal cord of individual mice provides insufficient material for RNA extraction, the mice were randomly divided into three groups and the samples in each group were pooled. A total of 10 normal spinal cords were randomly pooled to create three control groups, two of which contained 3 mice and one contained 4 mice.

Human subjects. Aborted NTD case subjects were obtained from Fenyang Hospital and Linxian County Hospital (Shanxi, China). The surgical details were, as previously described (14). The spinal cord tissues were used in the following experiments. A total of four NTD-affected fetuses and four age-matched controls were used in the present study. The clinical phenotypes of the four cases of NTD were as follows: One case of thoracic meningomyelocele (24 weeks gestation; female), one case of anencephalic and occipital encephalomeningocele (17 weeks gestation; female), and two cases of thoracic and lumbar spina bifida (20 and 26 weeks gestation, respectively; female). The present study was approved by the Committee of Medical Ethics at the Capital Institute of Pediatrics (SHERLLM2014002). Written informed consent was obtained from the parents on behalf of the fetuses.

RNA extraction and reverse transcription-quantitative polymerase chain reaction (RT-qPCR). Total RNA was isolated from the samples using TRIzol® (cat. no. 15596-026; Invitrogen; Thermo Fisher Scientific, Inc., Waltham, MA, USA) and was reverse transcribed using a First Strand cDNA Synthesis kit (cat. no. K1612; Beijing TransGen Biotech Co., Ltd., Beijing, China). The cDNA samples were analyzed using an Applied Biosystems 7500 Real-Time PCR system (Thermo Fisher Scientific, Inc.) and a 2X PCR UltraSYBR Mixture kit (cat. no. CW0956; CWBIO, Beijing, China) containing carboxy-X-rhodamine, according to the manufacturer's protocol. The expression levels of the target genes were normalized to glyceraldehyde 3-phosphate dehydrogenase (*Gapdh*). The fold change in expression was determined using the $2^{-\Delta\Delta Cq}$

Table I. Primers for reverse transcription-quantitative polymerase chain reaction analyses of *Wnt2b* and *Wnt7b* mRNA.

Gene	Primer (5'→3')
mWnt2b	F: CGAGGTGGCAAACATCCTAT
	R: CTTTGAAGGCTCCACTCCTG
mWnt7b	F: GGCTCCTTCCTACTCGCTCT
	R: GAGTGTGACTGGTGGGTGTG
Gapdh	F: TGTGTCCGTCGTGGATCTGA
	R: CCTGCTTCACCACCTTCTTGA

m, mouse; F, forward; R, reverse; *Gapdh*, glyceraldehyde 3-phosphate dehydrogenase.

method (16). The primer sequences designed using Primer 5 and provided by Thermo Fisher Scientific, Inc. are listed in Table I. The PCR thermocycling steps were as follows: 95°C for 10 min, then 40 cycles of 95°C for 15 sec, 60°C for 1 min and 72°C for 5 min.

Chromatin immunoprecipitation (ChIP) assays. A ChIP assay kit was purchased from Invitrogen (Thermo Fisher Scientific, Inc.; cat. no. 49-2024). Chromatin was prepared from targeted tissues and sonicated to DNA lengths between 300 and 500 bp. The following antibodies were used: Polyclonal anti-rabbit H3K4me (cat. no. ab106165; Abcam, Cambridge, UK), polyclonal anti-rabbit H3K4ac (cat. no. ab113672; Abcam) and anti-H3K27me3 (cat. no. 17-622; EMD Millipore, Billerica, MA, USA) antibodies. Alkaline phosphate-conjugated rabbit anti-immunoglobulin G (Beijing Zhongshan Golden Bridge Biotechnology Co., Ltd., Beijing, China)-treated chromatin immunoprecipitated samples served as a negative control. The antibodies were coupled with Dynabeads® Protein A/G (Thermo Fisher Scientific, Inc.; cat. no. 49-2024) at 4°C for 1 h, then chromatin was bound to the antibody-dynabeads complex at 4°C for 2 h. ChIP-qPCR analysis was performed using an ABI 7500 system (Applied Biosystems). The primers (Thermo Fisher Scientific, Inc.) used for ChIP-PCRs are listed in Table II. The relative enrichment of the histone modification was determined using the $2^{(input-Cq)}_{NTDs}/2^{(input-Cq)}_{control}$ method (14).

DNA methylation analyses. Following ultrasonic sonication (P-141008; Diagenode SA, Seraing, Belgium) of mouse and human spinal cord tissues, genomic DNA was extracted from the homogenates using a Genomic DNA Miniprep kit (Axygen Scientific, Inc., Union City, CA, USA). A total of 500 ng genomic DNA from each sample was bisulfite-treated using an EZ DNA Methylation-Gold™ kit (cat. no. D5005; Zymo Research, Irvine, CA, USA). The Sequenom MassARRAY platform (CapitalBio Corporation, Beijing, China) was used to perform quantitative methylation analysis of *Wnt2b* and *Wnt7b* (13). The primers used to detect DNA methylation levels of the target regions are presented in Table III.

Statistical analysis. Statistical analyses of the transcripts, histone modification enrichment and DNA methylation levels of *Wnt* genes were performed at least three times. Data were

Table II. Primer sequences for chromatin immunoprecipitation.

| Gene	Primer (5'→3')	RefSeq accession	Product size (bp)	Target region
Wnt2b-1	F: CGAGAGTGGGTGGGAGAAG	NM_009520	125	chr3:104765115-104765239
	R: GGACTCCTTTGGCCACACTG			
Wnt2b-2	F: GAAGTGTCCGCAACCCTCTC	NM_009520	103	chr3:104764911-104765013
	R: TCCTAGCGCCCTTCACTCA			
Wnt7b	F: CGGAGCCAATACGCAGCA	NM_001163633	100	chr15:85411511-85411610
	R: CCAAACAGGTGAAAGTACGCG			
WNT2B-1	F: GGGCGGTGATAGAAGTTGCT	NM_004185	122	chr1:113008796-113008917
	R: TCAGCTTTCCGAAGAAGGGC			
WNT2B-2	F: CCCAGTGGAGTCAGGAAAGG	NM_004185	141	chr1:113009674-113009814
	R: TGGCAACTTGGTGCACTGTA			
WNT7B	F: GAGACCACCCACTCCCATTG	NM_058238	145	chr22:46373432-46373576
	R: CCTGGGGGTTGTGGGAATCTC			

F, forward; R, reverse.
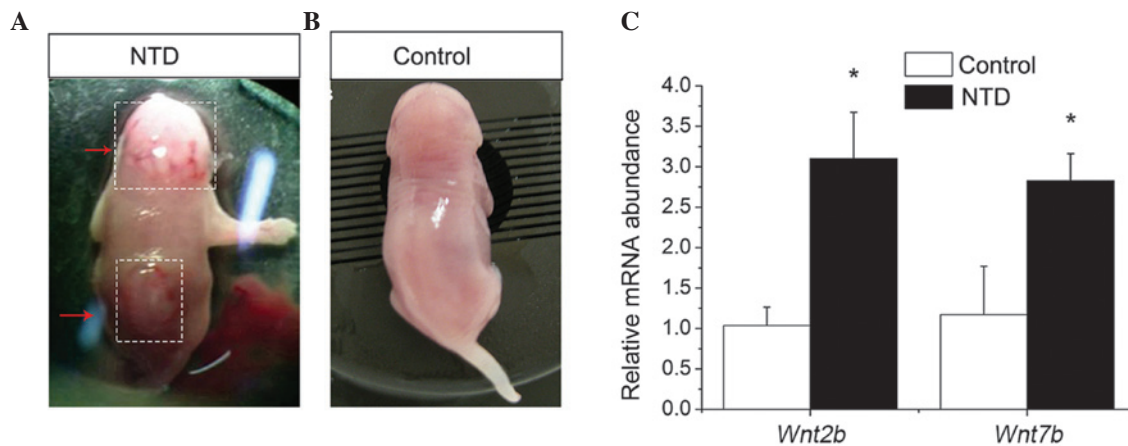
Figure 1. (A) RA-induced embryonic day 18.0 mouse embryos with typical exencephaly (top arrow) and spina bifida (bottom arrow), and (B) control mice. (C) Relative mRNA expression levels of *Wnt2b* and *Wnt7b* were significantly upregulated in the RA-induced mouse fetuses with NTDs, compared with the control group (*P<0.05). Data are presented as the mean ± standard error. RA, retinoic acid; NTD, neural tube defect.

compared between the test and control groups using Student's t-test with SPSS software, version 20 (IBM SPSS, Armonk, NY, USA). P<0.05 was considered to indicate a statistically significant difference.

Results

Altered transcription levels of Wnt2b and Wnt7b in a mouse model of RA-induced spina bifida. To determine into the possible changes occurring in the expression levels of *Wnt2b* and *Wnt7b* during the development of RA-induced NTDs, the mRNA expression levels were determined. The results indicated that, in the mice with spina bifida, the mRNA expression levels of *Wnt2b* and *Wnt7b* were 3.1- and 2.8-fold higher, respectively, compared with the control mice (Fig. 1C). These results were consistent with those of a previous study, which detected the transcriptional upregulation of *WNT2* (including *WNT2B*) and *WNT7B* in NT2/NTera2 cells following RA

treatment (17). These results indicated that the transcription of *Wnt2b* and *Wnt7b* were abnormally activated in RA-induced spina bifida.

Abnormal histone modifications are present in the promoter regions of Wnt2b and Wnt7b. Due to the ectopic alterations in mRNA expression levels, epigenetic factors in the GC-rich promoter regions of *Wnt2b* and *Wnt7b* were examined, according to the current UCSC database (July 2007 NCBI37/mm9; http://genome.ucsc.edu/). As shown in Fig. 2A and B, H3K4me3 and H3K27me3 modifications target *Wnt2b* and *Wnt7b* in embryonic stem cells and the brain in the central nervous system, whereas H3K9me3 modifications are weak. Furthermore, in the cerebellum and mouse embryonic fibroblasts, these histone modification enrichments are markedly lower, indicating that the histone modifications, which occur in *Wnt2b* and *Wnt7b* are stable and spatio-temporal specific. Therefore, the present study aimed to determine whether H3K27me3 or H3K4me bind

Table III. Primer sequences for DNA methylation.

Gene	Primer (5'→3')	RefSeq accession	Product size (bp)	Target region
Wnt2b-1	F: aggaagagagGGGAAAGTAGTTTAGTTTGTTTTTGA R: cagtaatacgactcactatagggagaaggctAAACTCCTTTAACCACACTACCCTC	NM_009520	349	chr3:104765115-104765463
Wnt2b-2	F: aggaagagagAGGGTAGTGTGGTTAAAGGAGTTTT R: cagtaatacgactcactatagggagaaggctCTTCCCTACCTACAACCCCCTAT	NM_009520	280	chr3:104764859-104765138
Wnt7b	F: aggaagagagTGAAGTGGTTAGGTTGGTTGGTAT R: cagtaatacgactcactatagggagaaggctACCTAAAAACCCAAACAAATAAAAAT	NM_001163633	205	chr15:85411502-85411706
WNT2B-1	F: aggaagagagGAAGGATAGGGTTAGTGGTTAGGAA R: cagtaatacgactcactatagggagaaggctAACCCCTTTTTAACAATTATAAACATCT	NM_004185	340	chr1:113008996-113009335
WNT2B-2	F: aggaagagagTTTTTTTTAGGGTTTGTGAGAATTT R: cagtaatacgactcactatagggagaaggctTTCCTAACCACTAACCCTATCCTTC	NM_004185	338	chr1:113008683-113009020
WNT2B-3	F: aggaagagagGATGGGGTTTTTAAGATTTAGGAGA R: cagtaatacgactcactatagggagaaggctACAAAAAAACAACAAAACCCATAAA	NM_004185	340	chr1:113008435-113008774
WNT2B-4	F: aggaagagagTTGTTATATTTGTTTGTGGAGGAGG R: cagtaatacgactcactatagggagaaggctAATCAAAATCTTCCTAAAAACACCC	NM_004185 NM_004185	268	chr1:113007526-113007793
WNT2B-5	F: aggaagagagTTTTGTTTTTATGTTTTTGAATAGG R: cagtaatacgactcactatagggagaaggctACCCCTTCCCAACAAAACTATTAT	NM_004185	328	chr1:113007314-113007641
WNT7B-1	F: aggaagagagGTTTTGGGGAGTAGGGGTTATTTA R: cagtaatacgactcactatagggagaaggctACTACCCTATCCCACCTAACCAAAC	NM_058238	326	chr22:46374152-46374477
WNT7B-2	F: aggaagagagGGGAGTTATTTAGGGTTGAGAAAGT R: cagtaatacgactcactatagggagaaggctACACTAAAAAAAACTCCTAACCCCC	NM_058238 NM_058238	318	chr22:46373742-46374059
WNT7B-3	F: aggaagagagGGTTAATGGGTTTTGTGAGGGTTA R: cagtaatacgactcactatagggagaaggctAAAAAACCACCCACTCCCATTAC	NM_058238 NM_058238	265	chr22:46373430-46373694

Upper case bases indicate the target region sequence, lower case bases indicate the probe sequence. F, forward; R, reverse.
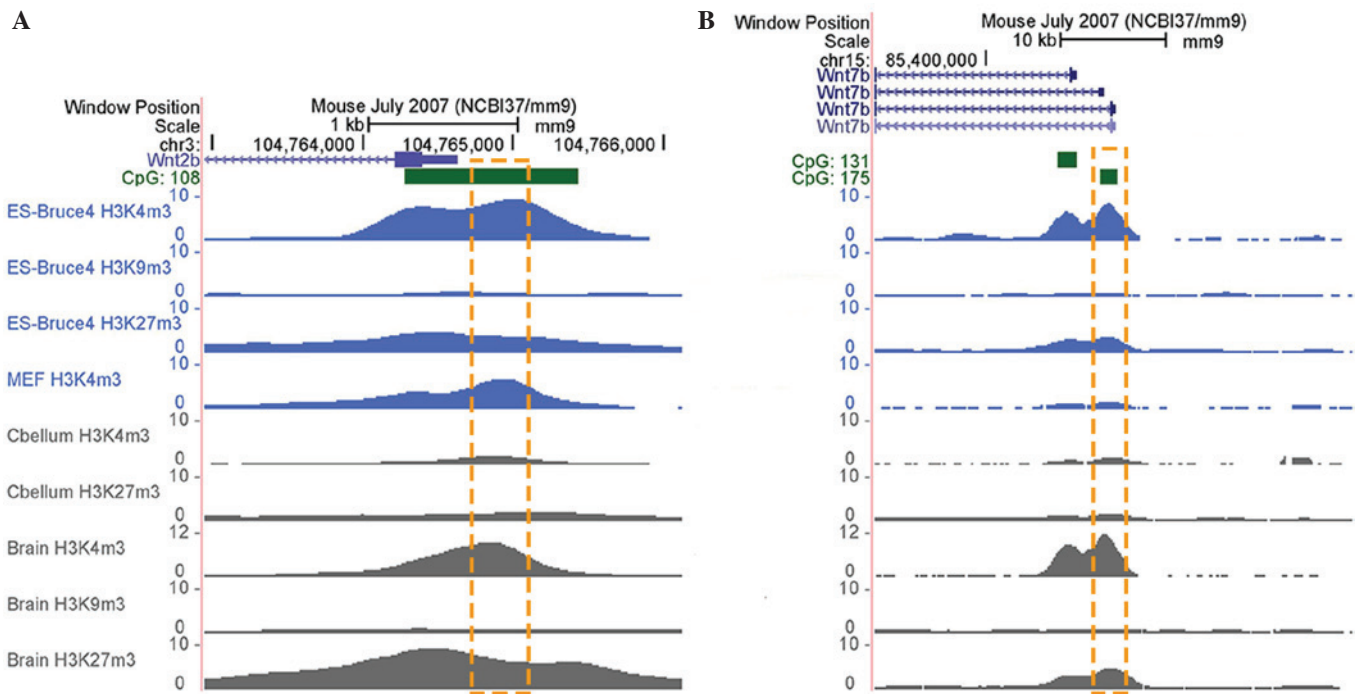
Figure 2. Histone modification enrichment profiles of *Wnt2b* and *Wnt7b* in mice. Browser shots from the UCSC genome browser showing H3K4me3, H3K9me3 and H3K27me3 ChIP-seq data in various tissues and cells. The positions of UCSC CpG islands (green) are shown. ChIP-seq data are presented as the number of reads that overlap genomic windows. In mice, H3K4me3 and H3K27me3 modification levels of (A) *Wnt2b* and (B) *Wnt7b* in ES cells and brain tissue were higher, compared with in the MEF and cerebellum; however, H3K9me3 modifications in these two *Wnt* genes in cells and tissues were low. Orange dotted box indicates the target regions of genes in the present study. H3K, histone 3 lysine; me3, trimethylation; ChIP, chromatin immunoprecipitation; ES, embryonic stem cell; MEF, mouse embryonic fibroblast.

to the target regions of samples by performing ChIP assays. As H3K4ac is also a transcriptional activation marker (18), the enrichment of this modification was also assessed. In the target regions of *Wnt2b* and *Wnt7b* in the RA-treated NTD mice, enrichments of H3K4ac were upregulated, whereas H3K27me3 enrichments were significantly downregulated in the chr3: 104765115-104765239 segment of *Wnt2b* (Fig. 3A). The enrichment of H3K4me was undetectable in the target regions of the two genes (data not shown). The abnormally attenuated H3K27me3 and enhanced H3K4ac enrichment of *Wnt2b* and *Wnt7b* indicated their roles in the dysregulated increased transcription observed in the mice with NTDs.

DNA methylation levels of Wnt2b and Wnt7b are abnormal in histone modification-enriched regions. Alterations in the histone modification profiles of the *Wnt* genes prompted the present study to examine DNA methylation in the histone modification-enriched regions. No difference was observed in the mean methylation levels of the target *Wnt2b* and *Wnt7b* regions between the NTD samples (*Wnt2b*, 5.36%; *Wnt7b*, 5.13%) and the control samples (*Wnt2b*, 5.79%; *Wnt7b*,4.93%; P=0.70 and P=0.92, respectively), as determined using the MassARRAY platform. However, the methylation levels of *Wnt2b* at the CpG-units chr3: 104765161-62 (-535 bp upstream from TSS) and chr3: 104765089-90 (-463 bp upstream from TSS) were significantly hypomethylated in the mice with spina bifida, compared with the controls (Fig. 3B and C). For *Wnt7b*, the chr15: 85411571-72 CpG site (407 bp upstream of the TSS) was also hypomethylated (Fig. 3D). These results suggested that, in NTDs, the increased mRNA expression levels of *Wnt2b*

and *Wnt7b* may also be partially due to hypomethylation of specific CpG-units in the promoter regions.

The combination of the ChIP assay and DNA methylation assay data suggested that, in the mouse model of RA-induced spina bifida, increased H3K4ac and decreased H3K27me3 enrichment, and hypomethylation of CpG islands in the promoter regions potentially led to enhanced mRNA expression (Fig. 4).

Aberrant epigenetic modification of WNT2B and WNT7B in human NTDs. As abnormal epigenetic modifications of *Wnt2b* and *Wnt7b* were detected in the mice with NTDs, the present study subsequently aimed to validate whether similar changes were present in the human NTD samples. In H1 embryonic stem cells, at the early stage prior to neural development, the GC-rich promoters of the two *WNT* genes were enriched for H3K27me3 (Fig. 5A and B), and were bound to a series of enzymes for its catalysis, including enhancer of zeste homolog 2 (EZH2) and suppressor of zeste homolog 12 (SUZ12). However, low levels of HDAC2-6 were detected, which is known to regulate the deacetylation of H3. Furthermore, astrocytes (NH-A), which are a type of mature neuronal cell associated with the later stage of neural development, exhibited reduced H3K27me3 and EZH2 enrichment (19), indicating that H3K27me3 and H3K4ac may preferentially function in the early stage of neural development.

In the human spinal cord samples, the GC-rich promoter regions of *WNT2B* and *WNT7B* were enriched for H3K4ac and H3K27me3. However, in the NTD samples, H3K4ac enrichment was downregulated, compared with the controls,
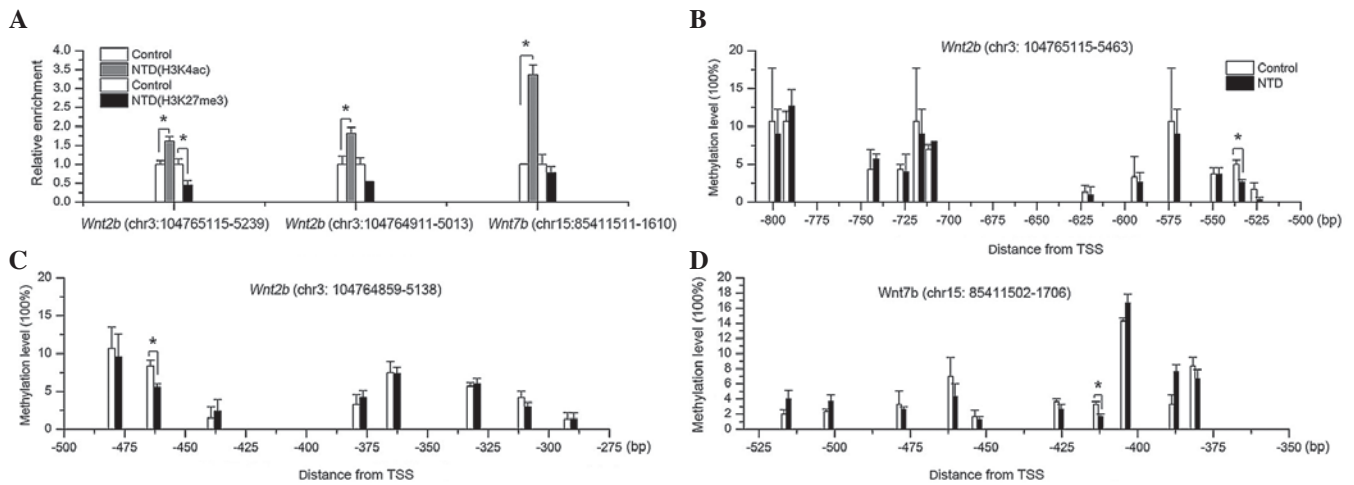
Figure 3. Alterations of epigenetic modification in NTDs. (A) In *Wnt2b*, H3K27me3 enrichment was decreased, whereas H3K4ac enrichment was increased in the promoter regions of *Wnt2b* and *Wnt7b*. DNA methylation levels of the specific CpG sites within (B and C) *Wnt2b* and (D) *Wnt7b* in a mouse model of retinoic acid-induced NTD, compared with in the control mice. *P<0.05; data are presented as the mean ± standard error. NTD, neural tube defect; H3K, histone 3 lysine; me3, trimethylation; ac, acetylation; TSS, transcription start site.
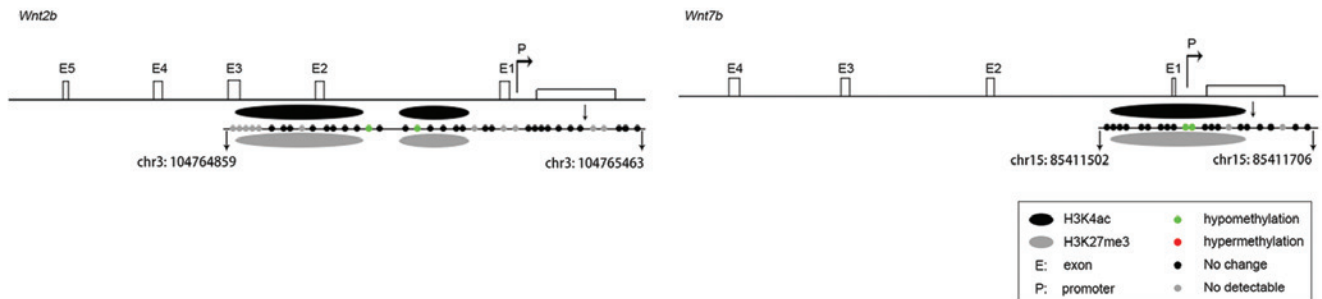
Figure 4. Schematic of H3K4ac, H3K27me3 and DNA methylation on target regions of *Wnt2b* and *Wnt7b* in mice H3K, histone 3 lysine; ac, acetylation; me3, trimethylation.

and there were no differences in H3K27me3 enrichment between the groups (Fig. 6A). Furthermore, several CpG-units of *WNT2B* and *WNT7B* were significantly hypomethylated, compared with the control group, particularly those close to the TSS (Figs. 6B-D and 7). These results indicated that aberrant epigenetic modification of *WNT2B* and *WNT7B* occurred in the human NTDs.

Discussion

Previous studies have demonstrated that H3K27me3 binding assists in maintaining gene silencing in multi-cellular organisms, and is associated with the timed suppression of developmental regulatory genes (20,21). By contrast, H3K4ac is considered to be involved in the activation of gene transcription (18), whereas methylated DNA makes it difficult for histones to form nucleosomes, resulting in chromosomal instability and modified accessibility of regulatory proteins, which alter the pattern of gene expression (12,22). The present study hypothesized that the aberrant DNA methylation and histone modification profiles observed in NTDs may affect the binding ability of RNA polymerase and key transcription factors to promoter regions on genes, including EZH2, SUZ12, HDAC2, HDAC6, which in turn regulate histone modification and affect transcription

initiation (19). In addition, H3K4ac and H3K27me3 modifications of the target genes in the present study were observed to function preferentially at the early stage of neural development, however not in the later stages. Furthermore, taking the data from our previous study into account, which reported DNA hypomethylation of long interspersed nuclear element-1 and low expression levels of H3K79me2 in human NTDs (13,14), the present study reiterates the hypothesis that abnormal epigenetic modifications have a destructive role in the etiology of NTDs.

It remains uncertain how alterations in *Wnt2b* and *Wnt7b* affect normal neural development. As ligands, *Wnt2b* and *Wnt7b* can function through the canonical β-catenin pathway, which maintains the proliferative state of neural progenitor cells (23,24). In addition, *Wnt7b* can signal through the non-canonical pathway (planar cell polarity), affect convergent extension movements prior to the closure of the neural tube, and control A/P axis formation and neural patterning (25). Therefore, the upregulated expression levels of *Wnt2b* and *Wnt7b* may lead to excessive signaling and result in disordered neural development, suggesting that aberrant *Wnt* gene expression may be involved in the etiology of NTDs. However, the *Wnt5a* genetic knockout mice demonstrated that individual deficiencies in *Wnt* genes do not induce an NTD phenotype (5). This suggests that,
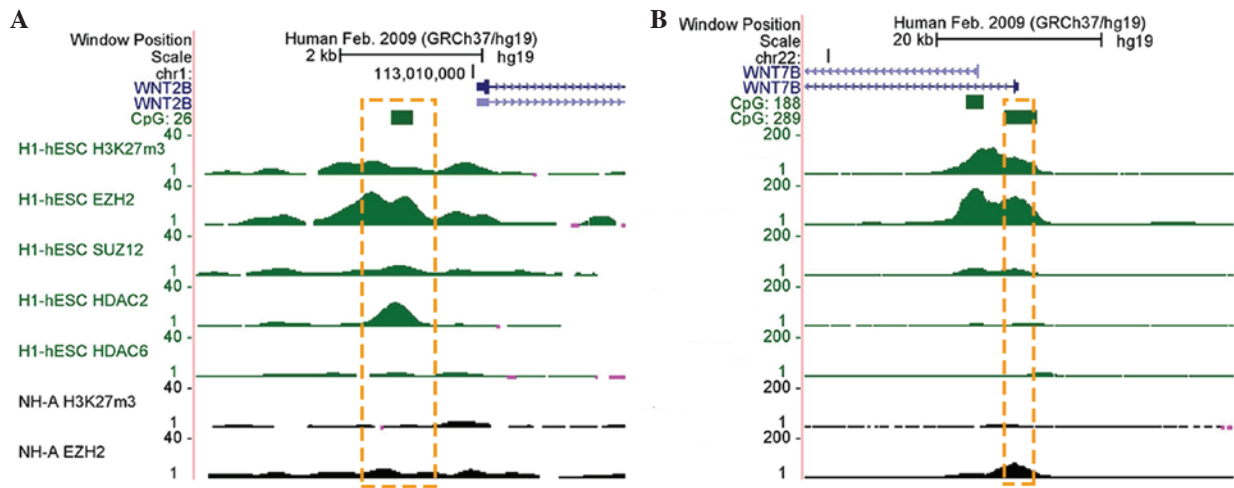
Figure 5. Histone modification enrichment profiles of *WNT2B* and *WNT7B* in humans. Browser shots from the UCSC genome browser showing H3K4me3, H3K9me3 and H3K27me3 ChIP-seq data in various tissues and cells. The positions of the UCSC CpG islands (green) are shown. ChIP-seq data is presented as the number of reads that overlap genomic windows. In humans, stable H3K27me3 modifications were detected in (A) *WNT2B* and (B) *WNT7B* in the ESCs, but not in NH-A. Orange dotted box indicates the target regions of genes in the present study. H3K, histone 3 lysine; me3, trimethylation; ChIP, chromatin immunoprecipitation; hESC, human embryonic stem cell; NH-A, astrocyte; EZH2, enhancer of zeste homolog 2; SUZ, suppressor of zeste homolog 12; HDAC, histone deacetylase.
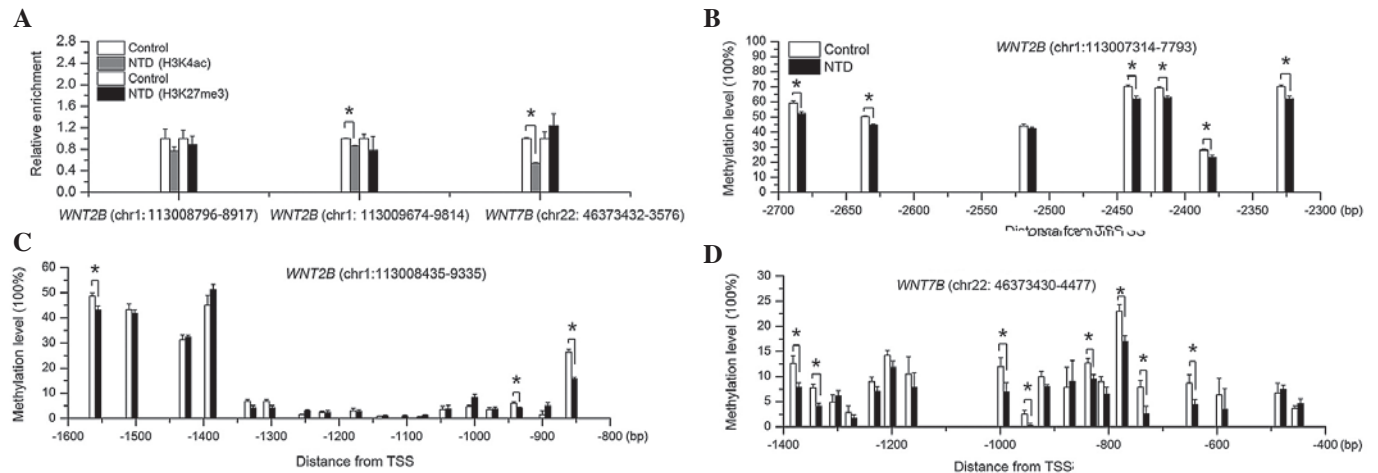

Figure 6. Alterations of epigenetic modification in human NTDs. (A) In *WNT2B* and *WNT7B*, H3K4ac enrichment was reduced in NTDs, whereas no differences in H3K27me3 modification were observed between the NTD and control groups. DNA methylation levels of the specific CpG sites within (B and C) *WNT2B* and (D) *WNT7B* target regions in human patients with NTDs, compared with in the controls. *P<0.05; data are presented as the mean ± standard error. NTD, neural tube defect; H3K, histone 3 lysine; me3, trimethylation; ac, acetylation; TSS, transcription start site.
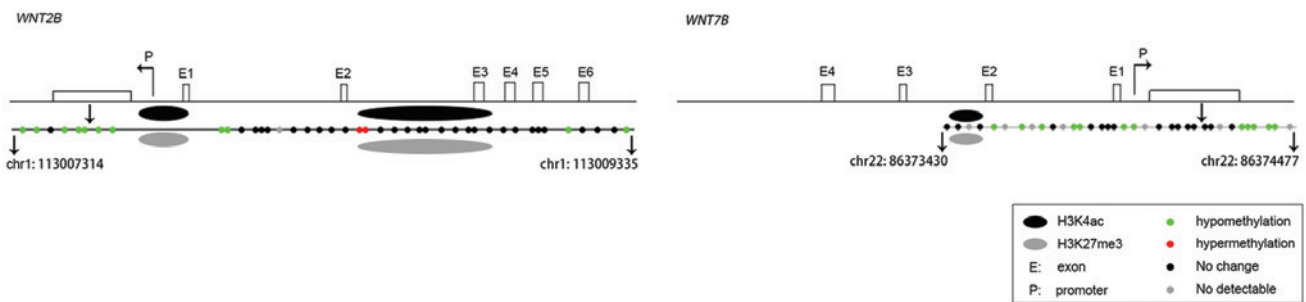

Figure 7. Schematic of H3K4ac, H3K27me3 and DNA methylation on target regions of *WNT2B* and *WNT7B* in human H3K, histone 3 lysine; ac, acetylation; me3, trimethylation.

when multiple *Wnt* ligands are altered at one time, they may potentially contribute to the etiology of disease. However, further studies are required to confirm this hypothesis.

In conclusion, the present study provided novel insight into the synergistic function of transcriptional dysregulation and epigenetic modifications. Specifically, abnormal epigenetic

modifications in the *Wnt* genes were detected following exposure to RA and may significantly contribute to the development and etiology of NTDs.

Acknowledgements

References

1. Mulligan KA and Cheyette BN: Wnt signaling in vertebrate neural development and function. J Neuroimmune Pharmacol 7: 774-787, 2012.
2. Carter M, Chen X, Slowinska B, Minnerath S, Glickstein S, Shi L, Campagne F, Weinstein H and Ross ME: Crooked tail (Cd) model of human folate-responsive neural tube defects is mutated in Wnt coreceptor lipoprotein receptor-related protein 6. Proc Natl Acad Sci USA 102: 12843-12848, 2005.
3. Copp AJ and Greene ND: Genetics and development of neural tube defects. J Pathol 220: 217-230, 2010.
4. Greco TL, Takada S, Newhouse MM, McMahon JA, McMahon AP and Camper SA: Analysis of the vestigial tail mutation demonstrates that Wnt-3a gene dosage regulates mouse axial development. Genes Dev 10: 313-324, 1996.
5. Qian D, Jones C, Rzadzinska A, Mark S, Zhang X, Steel KP, Dai X and Chen P: Wnt5a functions in planar cell polarity regulation in mice. Dev Biol 306: 121-133, 2007.
6. van Amerongen R and Berns A: Knockout mouse models to study Wnt signal transduction. Trends Genet 22: 678-689, 2006.
7. Kemp C, Willems E, Abdo S, Lambiv L and Leyns L: Expression of all Wnt genes and their secreted antagonists during mouse blastocyst and postimplantation development. Dev Dyn 233: 1064-1075, 2005.
8. Tsukiyama T and Yamaguchi TP: Mice lacking Wnt2b are viable and display a postnatal olfactory bulb phenotype. Neurosci Lett 512: 48-52, 2012.
9. Beretta CA, Brinkmann I and Carl M: All four zebrafish Wnt7 genes are expressed during early brain development. Gene Expr Patterns 11: 277-284, 2011.
10. Fenstermaker AG, Prasad AA, Bechara A, Adolfs Y, Tissir F, Goffinet A, Zou Y and Pasterkamp RJ: Wnt/planar cell polarity signaling controls the anterior-posterior organization of monoaminergic axons in the brainstem. J Neurosci 30: 16053-16064, 2010.
11. Ha M, Ng DW, Li WH and Chen ZJ: Coordinated histone modifications are associated with gene expression variation within and between species. Genome Res 21: 590-598, 2011.
12. Weber M, Hellmann I, Stadler MB, Ramos L, Pääbo S, Rebhan M and Schübeler D: Distribution, silencing potential and evolutionary impact of promoter DNA methylation in the human genome. Nat Genet 39: 457-466, 2007.
13. Wang L, Wang F, Guan J, Le J, Wu L, Zou J, Zhao H, Pei L, Zheng X and Zhang T: Relation between hypomethylation of long interspersed nucleotide elements and risk of neural tube defects. Am J Clin Nutr 91: 1359-1367, 2010.
14. Zhang Q, Xue P, Li H, Bao Y, Wu L, Chang S, Niu B, Yang F and Zhang T: Histone modification mapping in human brain reveals aberrant expression of histone H3 lysine 79 dimethylation in neural tube defects. Neurobiol Dis 54: 404-413, 2013.
15. Chen S, Bai B, Wang X, Li H and Zhang T: Retinoic acid induced neural tube defects in C57 mice in a dose-dependent and time-specific way. Chinese Journal of Birth Health & Heredity 122-124, 2014.
16. Zhang M, Shi J, Huang Y and Lai L: Expression of canonical WNT/β-CATENIN signaling components in the developing human lung. BMC Dev Biol 12: 21, 2012.
17. Katoh M: Regulation of WNT signaling molecules by retinoic acid during neuronal differentiation in NT2 cells: Threshold model of WNT action (review). Int J Mol Med 10: 683-687, 2002.
18. Xhemalce B and Kouzarides T: A chromodomain switch mediated by histone H3 Lys 4 acetylation regulates heterochromatin assembly. Genes Dev 24: 647-652, 2010.
19. Ram O, Goren A, Amit I, Shoresh N, Yosef N, Ernst J, Kellis M, Gymrek M, Issner R, Coyne M, *et al*: Combinatorial patterning of chromatin regulators uncovered by genome-wide location analysis in human cells. Cell 147: 1628-1639, 2011.
20. Nie Y, Liu H and Sun X: The patterns of histone modifications in the vicinity of transcription factor binding sites in human lymphoblastoid cell lines. PLoS One 8: e60002, 2013.
21. Voigt P, Tee WW and Reinberg D: A double take on bivalent promoters. Genes Dev 27: 1318-1338, 2013.
22. Eden A, Gaudet F, Waghmare A and Jaenisch R: Chromosomal instability and tumors promoted by DNA hypomethylation. Science 300: 455, 2003.
23. Cajánek L, Ribeiro D, Liste I, Parish CL, Bryja V and Arenas E: Wnt/beta-catenin signaling blockade promotes neuronal induction and dopaminergic differentiation in embryonic stem cells. Stem Cells 27: 2917-2927, 2009.
24. Wexler EM, Paucer A, Kornblum HI, Palmer TD and Geschwind DH: Endogenous Wnt signaling maintains neural progenitor cell potency. Stem Cells 27: 1130-1141, 2009.
25. Freese JL, Pino D and Pleasure SJ: Wnt signaling in development and disease. Neurobiol Dis 38: 148-153, 2010.